Bioorganic & Medicinal Chemistry 16 (2008) 9032–9039

Contents lists available at ScienceDirect

Bioorganic & Medicinal Chemistry

journal homepage: www.elsevier.com/locate/bmc

Peptidyl epoxides extended in the P′ direction as cysteine protease inhibitors: Effect on affinity and mechanism of inhibition

Nurit Perlman, Maya Hazan, Michael Shokhen, Amnon Albeck *

The Julius Spokojny Bioorganic Chemistry Laboratory, Department of Chemistry, Bar Ilan University, Ramat Gan 52900, Israel

ARTICLE INFO

Article history:
Received 4 August 2008
Revised 13 August 2008
Accepted 14 August 2008
Available online 19 August 2008

Keywords:
Peptidomimetics
Endo peptidyl epoxides
Enzyme inhibitors
Papain
Cathepsin B
Structure–activity relationships

ABSTRACT

Endo peptidyl epoxides, in which the central epoxidic moiety replaces the scissile amide bond of a P_3–P'_3 peptide, were designed as cysteine proteases inhibitors. The additional P′–S′ interactions, relative to those of an *exo* peptidyl epoxide of the same P_3–P_1 sequence, significantly improved affinity to the enzymes papain and cathepsin B, but also changed the mode of inhibition from active-site directed inactivation to reversible competitive inhibition. Computational models rationalize the binding affinity and the inhibition mechanism.

1. Introduction

Cysteine proteases emerge as an important target for the development of low-molecular-weight inhibitors.[1] Papain, the prototype cysteine endopeptidase, is probably the best studied enzyme in this family. Its amino acid sequence, 3D structure and substrate specificity are well studied. Seven substrate-recognition subsites, S_4–S'_3, were identified in papain, extending both sides of the scissile amide bond.[2] Some studies suggest that the substrate binding site is limited to the S_3–S'_2 subsites,[3] while another study confirmed an extended binding-site.[4] Nevertheless, most studies on papain dealing with both substrate specificity and enzyme inhibition have focused on the P–S interactions. Peptidyl aldehydes, trifluoromethanes, halomethanes, diazomethanes, nitriles, and epoxides illustrate this approach.[5] On the other hand, little attention has been paid to the P′–S′ interactions.[1b,6] In contrast, many peptide-based inhibitors spanning both P and P′ residues were developed for the other protease families—the serine-, aspartic-, and metallo proteases.[6g,7]

Thus, it would be of interest to apply the same principle of utilizing both P–S and P′–S′ interactions for the inhibition of cysteine proteases. Previous studies in our laboratory have shown that simple peptidyl epoxides, peptides that carry an epoxidic moiety at their C-terminal, are selective mechanism-based inactivators of cysteine proteases, alkylating the enzyme's active-site cysteine.[8] Correlation of peptide sequence selectivity with the known selectivity of the cysteine proteases examined indicated that the peptidyl epoxides bind to the enzyme 'normally'—occupying the enzyme's S subsites. In the present study, we explored the effect of extending the peptidyl epoxides to span P_3–P'_3 residues on the enzyme–inhibitor interactions.

A number of studies on the substrate sequence selectivity of papain suggest a large hydrophobic amino acid at the P_2 position and low specificity toward the P_1 residue, with Gly being one of the best possible residues. Gly, Ala or other small amino acids are preferred at the P'_1 and P'_2 position, and low specificity was observed for the P'_3 position.[3a,4] The latter position probably contributes binding interactions only by backbone amide hydrogen bonds.[3] Cathepsin B is a human abundant cysteine protease, involved in many biological activities. It is implicated in a variety of disease states such as inflammation and cancer.[9] Cathepsin B displays high sequence homology and 3D structure similarity to papain.[5d] Their substrate selectivity is also similar. Based on these studies, we designed the pentapeptide Cbz-Phe-Ψ[Gly-epoxy-Gly]-Ala-AlaOMe, spanning the P_2–P'_3 region (Scheme 1). The Cbz protecting group may occupy the S_3 subsite, thus extending the peptide to include P_3–S_3 interactions with the enzymes. The inhibitory activity of this peptide toward papain and cathepsin B would be compared with the corresponding activity of Cbz-Phe-Gly-epoxide (Scheme 1), an *exo* peptidyl epoxide that can interact only with the S_3–S_1 enzyme subsites.

* Corresponding author. Tel.: +972 3 5318862; fax: +972 3 7384053.
E-mail address: albecka@mail.biu.ac.il (A. Albeck).

0968-0896/$ - see front matter © 2008 Elsevier Ltd. All rights reserved.
doi:10.1016/j.bmc.2008.08.031

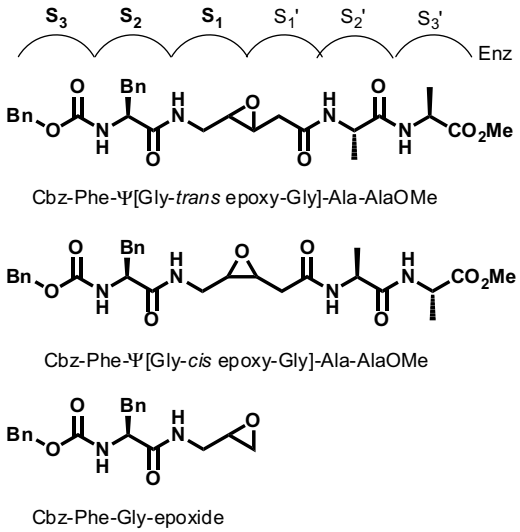

Scheme 1. The two *endo* peptidyl epoxides Cbz-Phe-Ψ[Gly-epoxy-Gly]-Ala-Ala-OMe **4** (*trans* and *cis*) and *exo* peptidyl epoxide Cbz-Phe-Gly-epoxide inhibitors and the corresponding papain subsites that interact with them.

2. Results and discussion

2.1. Synthesis

The synthesis of the *trans* and *cis* isomers of pentapeptidyl epoxide Cbz-Phe-Ψ[Gly-epoxy-Gly]-Ala-AlaOMe **4** is outlined in Scheme 2. The peptides were constructed from three parts. The two possible isomers (*trans* and *cis*) of the central Gly=Gly dipeptide olefin isostere, 5-amino-3-pentenoic acid, were stereoselectively synthesized separately. The *trans* isomer was prepared from the commercially available (*E*)-hex-3-enedioic acid by Schmidt rearrangement.[10] (*Z*)-hex-3-enedioic acid, required for the synthesis of the *cis* isomer, was prepared from 1,4-cyclohexadiene by three consecutive oxidation reactions.[11] This part of the peptide, corresponding to the P_1–P'_1 residues, was coupled to the N-terminal Cbz-phenylalanine residue (P_2), followed by coupling to the C-terminal Ala-Ala dipeptide (P'_2–P'_3). The resulting pentapeptidyl olefin **3** was then epoxidized to the final peptidyl epoxide **4**. As expected,[12] the epoxidation reaction was non stereoselective, yielding an almost 1:1 mixture of two diastereomers for each of the peptidyl olefins. All attempts to separate the two diastereomers by either reversed-, normal-, or chiral-phase HPLC under many different conditions failed. Probably the very small change in the position of a single oxygen atom, relative to a large peptide with three chiral centers, does not provide significant different diastereomeric interactions with the various stationary chromatographic phases for efficient separation. An attempt of stereoselective epoxidation[13] also failed, probably due to similar reasons.

The P_2–P_1 *exo* peptidyl epoxide, Cbz-Phe-Gly-epoxide was prepared, as a 1:0.8 mixture of isomers, according to a published procedure.[14]

2.2. Biological activity

The *exo* peptidyl epoxide, Cbz-Phe-Gly-epoxide, exhibited time- and concentration-dependent inhibition of the cysteine proteases

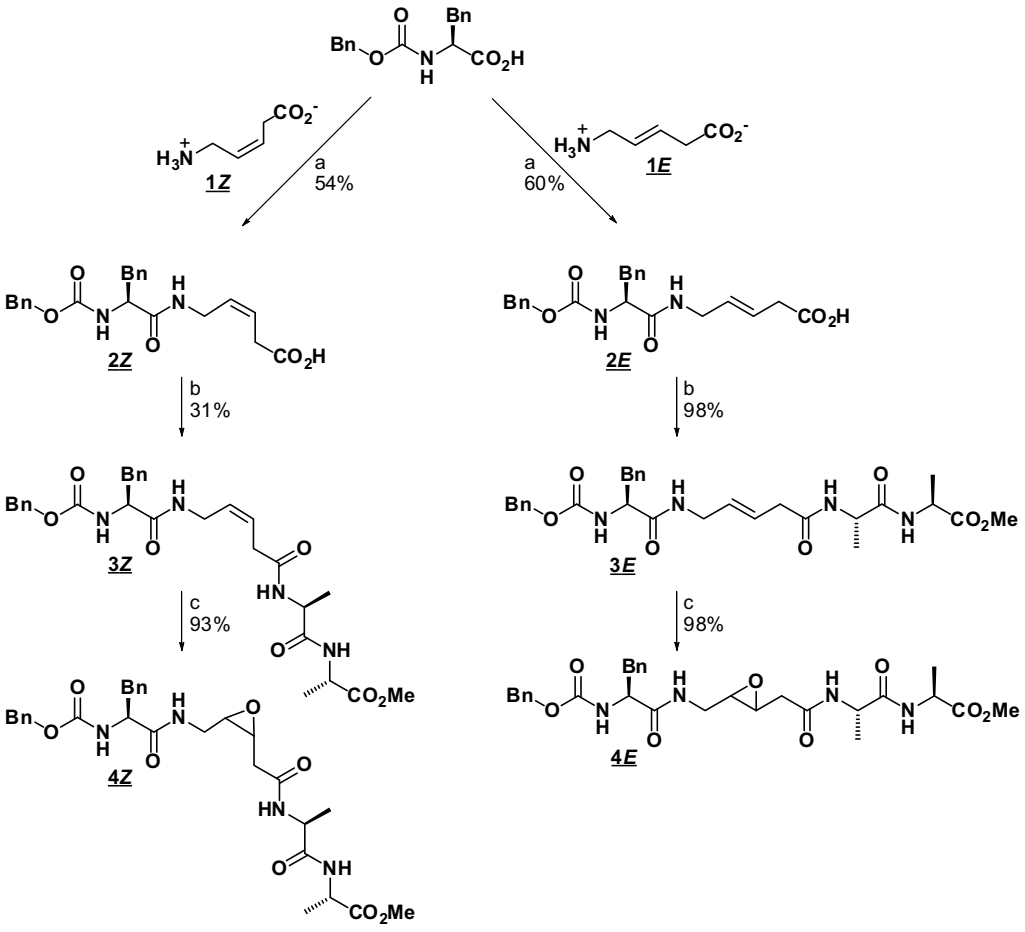

Scheme 2. Synthesis of pentapeptidyl epoxide Cbz-Phe-Ψ[Gly-epoxy-Gly]-Ala-AlaOMe **4**. Reagents: (a) DCC, NHS, THF; (b) HCl·Ala-AlaOMe, PyBOP, Et_3N, THF; (c) *m*-CPBA, CH_2Cl_2.

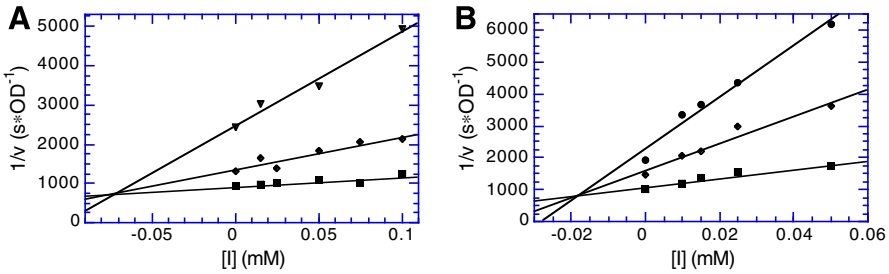

Figure 1. Papain inhibition by endo peptidyl epoxides. A Dixon plot[15] for the inhibition of papain-catalyzed hydrolysis of Cbz-Glycine p-nitrophenyl ester by (A) Cbz-Phe-Ψ[Gly-*trans* epoxy-Gly]-Ala-AlaOMe and (B) Cbz-Phe-Ψ[Gly-*cis* epoxy-Gly]-Ala-AlaOMe. Assay conditions: 100 mM phosphate buffer, pH 7.1, 25 °C, [enzyme] = 5×10^{-8} M. The substrate (final concentration: ■, 100 μM; ♦, 40 μM; ●, 25 μM; ▼, 15 μM) and the inhibitor were introduced in acetonitrile, whose total concentration was 3% in the aqueous assay solution. The hydrolysis was monitored at 404 nm (ε 9000 M^{-1} cm^{-1}).

papain and cathepsin B, an indication of covalent (alkylation) interaction with the enzymes. This is in agreement with previous studies with similar peptidyl epoxides.[8a] The kinetic parameters determined to be $k_i = 10^{-2}$ min^{-1} and $K_i = 0.39$ mM for papain and $k_i = 3 \times 10^{-2}$ min^{-1} and $K_i = 1.02$ mM for cathepsin B. We expected that the addition of binding interactions at the P′–S′ side for a peptidyl epoxide spanning the P_3–P'_3 residues would result in a lower K_i value, and a better inactivator of the enzymes. Thus, the interaction of both *trans*- and *cis*-*endo* pentapeptidyl epoxide Cbz-Phe-Ψ[Gly-epoxy-Gly]-Ala-AlaOMe **4** with papain and cathepsin B was studied.

Contrary to the expectation, no time dependent loss of enzymatic activity was observed when the *endo* peptidyl epoxides (either *trans* and *cis*) were incubated with either papain or cathepsin B for up to two hours, both at 25 °C and at 37 °C. Instead, the compounds exhibited reversible competitive inhibition of the enzymes (Fig. 1 and Table 1). This mode of inhibition was further demonstrated by the full recovery of the enzymatic activity upon dialysis (in comparison with free active enzyme which underwent similar dialysis).

The extended peptide chain significantly increased the affinity of the inhibitor to the enzymes. Papain binds the *trans endo* peptidyl epoxide five times and the *cis endo* peptidyl epoxide twenty two times tighter than it binds the *exo* peptidyl epoxide, Cbz-Phe-Gly-epoxide, of the same P_3–P_1 sequence. Cathepsin B inhibition exhibited a similar trend (4- and 11-fold increased binding affinity of the *trans* and *cis endo* peptidyl epoxides, respectively). This can be explained mainly by the additional hydrogen bonds between the inhibitor backbone amides and the enzyme's residues or backbone.[16] It is interesting to note that the *cis* epoxy inhibitor has a higher affinity to papain and cathepsin B than the *trans* epoxy peptide has (4- and 3-fold lower K_i, respectively).

The most striking character of the *endo* peptidyl epoxide is the unexpected change of mechanism from mechanism-based irreversible inactivation of cysteine proteases by the *exo* (P_3–P_1) peptidyl epoxides to reversible competitive inhibition.[17] Similar results were previously observed, though the mode of binding was not clear.[18] On the other hand, a similar *cis* peptidyl epoxide irreversibly inactivated the HIV aspartic protease, demonstrating the intrinsic ability of such an epoxide to alkylate an enzyme active-site residue.[7d] It should also be noted that much data on the binding of epoxysuccinyl peptides in both the S and S′ sites of cysteine proteases is available,[6c,6d,6g] but these inhibitors bind in a reversed mode in the enzyme's S sites, and they are mechanistically distinct from simple peptidyl epoxides.[8b] This is also true for diaminoketone inhibitors[6e,6f] and some acyloxymethyl ketone inhibitors,[6g] which bind in the S′ sites in the reversed direction. The latter are also irreversible inhibitors of cysteine proteases.

Table 1
Dissociation constants (in μM) of peptidyl epoxide inhibitors from the non-covalent complexes with the cysteine proteases papain and cathepsin B

Inhibitor	K_i for papain	K_i for cathepsin B
Cbz-Phe-Ψ[Gly-epoxide][a]	390	1018
Cbz-Phe-Ψ[Gly-*trans* epoxy-Gly]-Ala-AlaOMe	73	244
Cbz-Phe-Ψ[Gly-*cis* epoxy-Gly]-Ala-AlaOMe	18	94

[a] Cbz-Phe-Ψ[Gly-epoxide] is an irreversible inhibitor, with k_i values of 1×10^{-2} and 3×10^{-2} min^{-1} toward papain and cathepsin B, respectively.

The failure of the *endo* peptidyl epoxide to alkylate the active-site cysteine may be the result of steric hindrance at the epoxide moiety. In this respect, it is interesting to note that the *exo* peptidyl epoxides alkylate the active-site cysteine by their epoxidic *exo* methylene rather than by the *endo* carbon, which corresponds to a substrate's carbonyl carbon.[8c] This may be the result of much better accessibility of the *exo* carbon to the nucleophilic thiol group. In the *endo* peptidyl epoxides, both epoxidic carbons are tertiary and therefore nucleophilic attack may be excluded for the same reason. Another possible explanation for the difference in mechanism is the relative free rotation of the small epoxidic group of the *exo* peptidyl epoxide in the enzyme active-site, compared with the rigidity of the epoxidic moiety in the extended *endo* peptidyl epoxide. This rigidity prevents the epoxide to be oriented in the right position to alkylate the enzyme's active-site cysteine (or other possible active-site nucleophiles). Thus, *endo* peptidyl epoxides exhibit higher affinity to cysteine proteases than the corresponding *exo* peptidyl epoxides, due to the additional P′–S′ interactions. These interactions confer rigidity of the peptide backbone, which precludes alkylation of the enzyme and, therefore, affects a change in the mechanism of inhibition.

2.3. Computational modeling

The above results pose a few questions: how are the inhibitors bound in the enzyme–inhibitor reversible complex, that is, do they occupy the enzyme's S_2–S'_3 sites? What is the reason for the change in inhibition mechanism? Do the enzymes preferentially bind only one of the two *cis* and one of the two *trans* diastereomers? In order to address these issues, we conducted a molecular modeling study to examine the alignment of the four inhibitors in the active site of papain, and to estimate their relative enzyme–inhibitor binding energies.[19]

The enzyme–inhibitor complexes were generated from the 2cio.pdb structure, applying the Yasara Dynamics software to introduce the structure of the desired inhibitors.[20] The structures were optimized by molecular dynamic (MD) simulations. Figure 2 presents one such structure of papain with a *cis* epoxy inhibitor. The inhibitor is well aligned in the enzyme active site, occupying the enzyme's S_2–S'_3 sites. A close-up view of the active site clearly shows that the orientation of the epoxide moiety relative to the catalytic cysteine prevents the nucleophilic attack of the latter. The S–C–O angle between the nucleophilic cysteine sulfur and the epoxidic carbon and oxygen is approximately 60° (Fig. 3). In

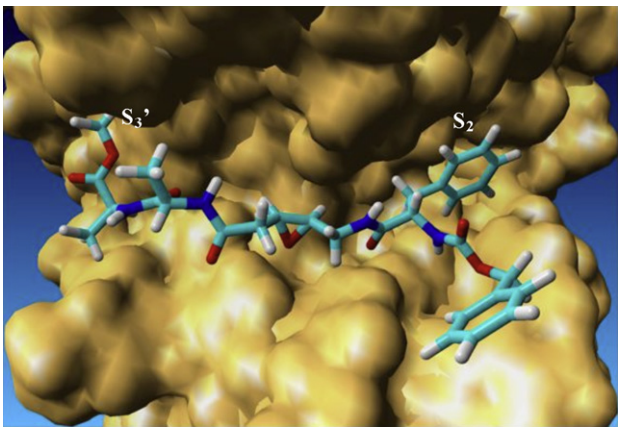

Figure 2. Inhibitor docked in the enzyme active site. Alignment of one of the two Cbz-Phe-Ψ[Gly-*cis* epoxy-Gly]-Ala-AlaOMe compounds in the S_2 (right)–S'_3 (left) active site of papain, obtained by molecular dynamic simulation. The enzyme is presented by its surface area, while the inhibitor is presented by sticks. Color scheme: C, cyan; H, white; N, blue; O, red. The figure was generated by the Yasara software.

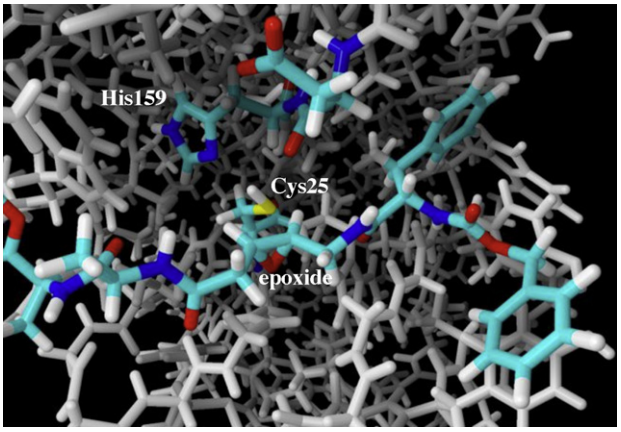

Figure 3. Close-up view of the inhibitor in the enzyme active site. A few enzyme residues, including the catalytic Cys25 and His159, are also color coded. Cys25 is located just behind the epoxide.

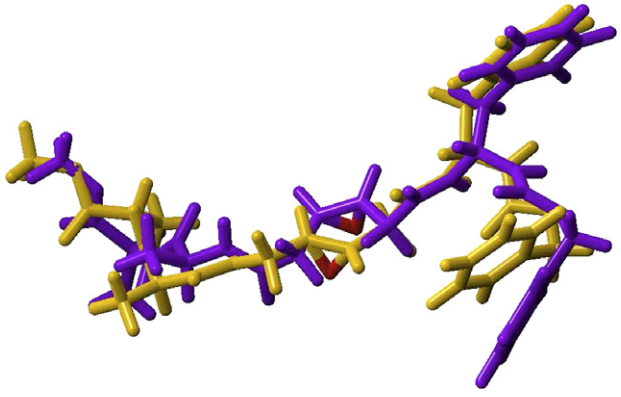

Figure 4. Superposition of *cis* and *trans endo* peptidyl epoxides. Superposition of one Cbz-Phe-Ψ[Gly-*cis* epoxy-Gly]-Ala-AlaOMe inhibitor (Fig 2) (purple) and the (*S*,*S*) Cbz-Phe-Ψ[Gly-*trans* epoxy-Gly]-Ala-AlaOMe (yellow) in the enzyme active site is shown. The epoxidic oxygens are colored in red. Both structures are derived from the corresponding MD optimized enzyme–inhibitor complexes by superposition of the protein backbone atoms of the two complexes, followed by removal of the protein atoms.

the *exo* peptidyl epoxide, on the other hand, rotations about the C–N and C–C bonds adjacent to the epoxidic moiety can place the epoxide carbon in the right position to covalently interact with the catalytic cysteine. It explains the change of inhibition mechanism from covalent inactivation by *exo* peptidyl epoxides to non-covalent competitive inhibition by the *endo* peptidyl epoxides. The epoxide functionalities in the other three structures are also oriented in such a way that prevents alkylation of the catalytic cysteine.

It is interesting to note the almost perfect superposition of the *cis* epoxide and the (*S*,*S*) *trans* epoxide in the enzyme active site (Fig. 4), which explains the relative small difference in the dissociation constants of the two isomers from their respective enzyme–inhibitor complexes.

The inhibitor binding energies to papain were estimated on large molecular clusters (about 600 atoms), sub-structures of the entire enzyme–inhibitor complexes that contain the inhibitors and the active-site residues of the enzyme. We applied semiempirical quantum mechanical (QM) calculations for the estimation of the binding trend of the four inhibitors. This approach has been applied for calculations of binding enthalpies for different enzymes.[21] Our calculations reproduced the higher affinity of the *cis* epoxide to papain, relative to the affinity of the *trans* isomer. The calculations indicate that one *cis* peptidyl epoxide (presented in Figs. 2 and 3) is bound to the enzyme by 1.5 kcal/mol tighter than the other *cis* epoxide. This difference in binding energy would be manifested in binding ratio of 92.5:7.5. Likewise, one *trans* epoxide, the (*S*,*S*) isomer, is 3.3 kcal/mol more tightly bound to the enzyme than its (*R*,*R*) *trans* counterpart, corresponding to 99.6:0.4 binding ratio. Thus, for both the *cis* and the *trans* epoxides, practically just one diastereomer is bound to the enzyme. This also implies that the actual dissociation constants are about half of the apparent values presented in Table 1.

3. Conclusions

Exo peptidyl epoxides are mechanism-based selective cysteine protease inactivators. Here we demonstrated that *endo* peptidyl epoxides, which may utilize both P–S and P′–S′ interactions with the target enzyme, indeed exhibited lower dissociation constant toward two cysteine proteases, in comparison with a corresponding *exo* peptidyl epoxide, which can only enjoy P–S interactions. Surprisingly, the *endo* peptidyl epoxide exhibited reversible competitive inhibition of the cysteine proteases, in contrast with the *exo* peptidyl epoxides, which are irreversible inactivators of the enzymes.

Our molecular modeling of the inhibition of cysteine proteases by *endo* peptidyl epoxides shed some light on this interaction. It suggests that the inhibitors indeed occupy the S_2–S'_3 enzyme binding sites, as expected. The epoxide moieties in all four stereoisomers are held by the rigid framework of the peptide in an orientation that does not enable alkylation of the catalytic thiol. Finally, energetic calculations predict that only one *cis* epoxide and one *trans* epoxide bind the enzyme, demonstrating highly stereoselective interaction between the enzyme and the inhibitors in the non-covalent complex.

4. Experimental

4.1. General

Anhydrous THF was dried and freshly distilled from sodium/benzophenone. TLC was performed on E. Merck 0.2 mm precoated silica gel F-254 plates, and viewed by UV light or Cl_2/KI-tolidine.[22] Flash column chromatography was carried out on silica gel 60

(230–400 mesh ASTM, E. Merck). ^{1}H and ^{13}C NMR spectra were recorded at 600 or 300 MHz and 150 or 75 MHz, respectively. ^{1}H NMR assignments were supported by homonuclear COSY experiments. ^{13}C NMR assignments were supported by DEPT or 2D hetero COSY experiments. *J* values are given in Hz. Mass spectra were recorded in DCI mode with methane as the reagent gas. HPLC of final peptidyl epoxides were carried out on a normal-phase silica column (Purospher-star 150 × 4 mm, 5 μm, Merck, with different 0–7% *i*PrOH in hexane gradients at 1 ml/min), a reversed-phase column (C18 Nucleosil 120 × 5 mm, 5 μm, Macherey-Nagel, at 1 ml/min) and on a chiral column (Chira Grom 250 × 2 mm, 5 μm, Altech, with different 0–5% *i*PrOH or 1–3% EtOH in hexane gradients at 0.3 ml/min). Papain (EC 3.4.22.2), its substrate Cbz-Gly-ONp, protected amino acids and peptides were from Sigma.

4.2. Synthesis

4.2.1. (*E*)- or (*Z*)-5-Aminopent-3-enoic acid (1)

Trans or *cis*-3-hexenedioic acid[11] was subjected to Schmidt reaction.[10] The diacid (1.4 g, 9.7 mmol) was suspended in chloroform (40 ml), and concentrated sulfuric acid (4.0 ml) was added. Sodium azide (0.65 g, 10 mmol) was added in small amounts over 30 min while the mixture was stirred rapidly. After further 4 h at 40 °C the chloroform layer was decanted from the viscous residue, which was washed again with chloroform (30 ml). The organic layers were washed also with distilled water (40 ml). The water from the washing was added to the acid layer that was dissolved in distilled water (110 ml) and added to a column of Dowex 50 W (H^+) ion-exchange resin (50 ml). The column was washed with water to neutral pH and then the amino acid was eluted with aqueous pyridine (300 ml, 1 M). Evaporation of the solvent afforded the product (58% and 38% yield for the *trans* and *cis* isomers, respectively).

4.2.1.1. (Z) 5-Aminopent-3-enoic acid. ^{1}H NMR (D_2O) δ 3.14 (d, ***J*** = 7.5 Hz, 2H, CH_2CO); 3.66 (d, ***J*** = 7.2 Hz, 2H, NCH_2); 5.67 (dt, ***J*** = 10.8, 7.2 Hz, 1H CH=); 5.96 (dt, ***J*** = 10.8, 7.5 Hz, 1H, =CH); ^{13}C NMR: δ 36.36, 36.63 (CH_2); 122.88, 131.98 (CH=CH); 179.66 (CO_2); HRMS: ***m/z*** 116.0711 (MH^+. $C_5H_{10}NO_2$ requires 116.0712).

4.2.1.2. (E) 5-Aminopent-3-enoic acid. ^{1}H NMR (D_2O): δ 2.97 (d, ***J*** = 7.2 Hz, 2H, CH_2CO); 3.55 (d, ***J*** = 6.6 Hz, 2H, NCH_2); 5.59 (dt, ***J*** = 15.6, 6.9 Hz, 1H CH=); 5.95 (dt, ***J*** = 15.3, 7.2 Hz, 1H, =CH); ^{13}C NMR: δ 41.53, 41.63 (CH_2); 123.71, 133.59 (CH=CH); 180.64 (CO_2); HRMS: ***m/z*** 116.0720 (MH^+. $C_5H_{10}NO_2$ requires 116.0712).

4.2.2. HCl·Ala-Ala-OCH_3

Acetyl chloride (1.08 ml, 15 mmol) was added dropwise via a reflux condenser to Ala-Ala (0.539 g, 3.36 mmol) in methanol (29 ml) at 0 °C. The condenser was removed and the solution was stirred over night. Evaporation of the solvent gave the product in 100% yield. ^{1}H NMR (CD_3OD): δ 1.38 (d, *J* = 7.3 Hz, 3 H, $CHCH_3$); 1.50 (d, *J* = 7.0 Hz, 3H, $CHCH_3$); 3.67 (s, 3H, OCH_3); 3.97 (q, *J* = 7.0 Hz, 1H, CH); 4.41 (q, *J* = 7.3 Hz, 1H, CH); ^{13}C NMR (D_2O with acetone as ref.): δ 16.47, 17.08 ($CHCH_3$); 49.40 (CH); 49.50 (OCH_3); 53.61 (CH); 171.20, 175.31 (CON,CO_2).

4.2.3. Coupling 1

N-Cbz-Phe (0.907 g, 3.0 mmol), DCC (0.783 g, 3.8 mmol) and NHS (0.706 g, 6.1 mmol) were stirred in THF (20 ml) at rt. After 2 h a solution of (*E*)- or (*Z*)-5-amino-3-pentenoic acid (0.432 g, 3.8 mmol) and sodium carbonate (0.664 g, 4.9 mmol) in water (5 ml) was added and the reaction mixture was stirred over night. The reaction mixture was filtered to remove the precipitation, ether (20 ml) was added and extracted with saturated Na_2CO_2. The aqueous layer was acidified with concd HCl. A white solid was participated and filtered in the *trans* reaction (60% yield). In the *cis* reaction, the aqueous phase was extracted with EtOAc (3× 50 ml). The organic layer was dried over $MgSO_4$ and evaporated to dryness (54% yield). The product was transferred to the next reaction without further purification.

4.2.3.1. (Z) $PhCH_2OCONHCH(CH_2Ph)CONHCH_2CH{=}CHCH_2CO_2H$ (cis Cbz-Phe-Gly=Gly) (2). ^{1}H NMR (CD_3OD): δ 2.86 (d, ***J*** = 6.9 Hz, 1H, $CHCH_2Ph$); 3.07 (m, 1H, $CHCH_2Ph$); 3.13 (dd, ***J*** = 7.5, 1.2 Hz, 2H, CH_2CO); 3.78 (m, 2H, NCH_2); 4.32 (td, ***J*** = 7.5, 7.2 Hz, 1H, NCH); 4.99 (d, ***J*** = 12.3, 1H, $PhCH_2O$); 5.05 (d, ***J*** = 11.7 Hz, 1H, $PhCH_2O$); 5.42 (dt, ***J*** = 10.8, 7.1 Hz, 1H, CH=); 5.67 (dtt, ***J*** = 10.8, 7.4, 1.4 Hz, 1H, =CH); 7.20–7.34 (m, 10H, Ph); ^{13}C NMR: δ 33.62 (CH_2CO); 37.38 (NCH_2); 39.34 (CH_2Ph); 58.02 (NCH); 67.58 ($PhCH_2O$); 125.87, 127.76, 128.72, 128.95, 129.23, 129.44, 130.36, 138.14, 138.45 (Ph, CH=CH); 158.14 (OCON); 173.75, 175.33 (CON, CO_2); HRMS: ***m/z*** 397.1740 (MH^+. $C_{22}H_{25}N_2O_5$ requires 397.1763).

4.2.3.2. (E) $PhCH_2OCONHCH(CH_2Ph)CONHCH_2CH{=}CHCH_2CO_2H$ (trans Cbz-Phe-Gly=Gly) (2). ^{1}H NMR (acetone-d_6): δ 2.94 (dd, ***J*** = 13.7, 8.9 Hz, 1H, $CHCH_2Ph$); 3.03 (d, ***J*** = 6.6 Hz, 2H, CH_2CO); 3.16 (dd, ***J*** = 13.8, 5.7 Hz, 1H, $CHCH_2Ph$); 3.77 (dd, ***J*** = 15.5, 5.6 Hz, 1H, NCH_2); 3.81 (dd, ***J*** = 15.9, 5.7 Hz, 1H, NCH_2); 4.43 (td, ***J*** = 8.7, 5.7 Hz, 1H, NCH); 4.97 (d, ***J*** = 12.6, 1H, $PhCH_2O$); 5.03 (d, ***J*** = 12.6 Hz, 1H, $PhCH_2O$); 5.53 (dt, ***J*** = 15.6, 5.7 Hz, 1H, CH=); 5.67 (dtt, ***J*** = 15.6, 6.6, 1 Hz, 1H, =CH); 6.49 (d, ***J*** = 8.4 Hz, 1H, $NHCH$); 7.20–7.40 (m, 10H, Ph); 7.46 (t, ***J*** = 6.7 Hz, 1H, $NHCH_2$); ^{13}C NMR; δ 37.65 (CH_2CO); 39.11 (CH_2Ph); 41.33 (NCH_2); 57.30 (NCH); 66.61 ($PhCH_2O$); 125.21, 127.25, 128.44, 129.04, 129.43, 130.21, 130.57, 138.14, 138.64 (Ph, CH=CH); 156.71 (OCON); 171.65, 172.67 (CON, CO_2); HRMS: ***m/z*** 397.1736 (MH^+. $C_{22}H_{25}N_2O_5$ requires 397.1763).

4.2.4. Coupling 2

HCl·Ala-Ala-OCH_3 (0.707 g, 3.36 mmol) in 5 ml THF and Cbz-Phe-Gly=Gly (0.610 g, 1.54 mmol) in 15 ml CH_2Cl_2 were stirred at rt. Et_3N was added (3 ml, 21.7 mmol), followed by PyBOP and the solution stirred over night. EtOAc (150 ml) was added and extracted with sat. $NaHCO_3$ (2× 100 ml), water (100 ml), HCl 1 M (2× 50 ml) and water (100 ml). The organic phase was then dried over $MgSO_4$ and evaporated, and the product was purified by flash chromatography (EtOAc/hexane a gradient from 1:1 to 9:1, 98% yield for the *trans* isomer and 31% yield for the *cis* isomer).

4.2.4.1. (Z) $PhCH_2OCONHCH(CH_2Ph)CONHCH_2CH{=}CHCH_2CONHCH(CH_3)CONHCH(CH_3)CO_2CH_3$ (cis Cbz-Phe-Gly=Gly-Ala-Ala-OCH_3) (3). ^{1}H NMR (CD_3OD): δ 1.36 (d, ***J*** = 7.2 Hz, 3H, $CHCH_3$); 1.36 (d, ***J*** = 7.2 Hz, 3H, $CHCH_3$); 2.82 (dd, ***J*** = 13.6, 8.8 Hz, 1H, $CHCH_2Ph$); 3.08 (m, 3H, $CHCH_2Ph{+}CH_2CO$); 3.69 (s, 3H, OCH_3); 3.79 (dd, ***J*** = 13.8, 5.9 Hz, 1H, NCH_2); 3.82 (dd, ***J*** = 13.8, 5.8 Hz, 1H, NCH_2); 4.32 (dd, ***J*** = 8.4, 6.4 Hz, 1H, $NHCHCH_2$); 4.35 (q, ***J*** = 7.1 Hz, 1H, $CHCH_3$); 4.40 (q, ***J*** = 7.3 Hz, 1H, $CHCH_3$); 5.00 (d, ***J*** = 12.6 Hz, 1H, $PhCH_2O$); 5.05 (d, ***J*** = 12.5 Hz, 1H, $PhCH_2O$); 5.45 (dt, ***J*** = 10.4, 6.0 Hz, 1H, CH=); 5.65 (dt, ***J*** = 11.2, 6.0 Hz, 1H, =CH); 7.20–7.34 (m, 10H, Ph); ^{13}C NMR : δ 17.34, 18.13 ($CHCH_3$); 35.37 (CH_2CO); 37.35 (NCH_2); 39.34 (CH_2Ph); 49.40, 50.24 ($CHCH_3$); 52.74 (OCH_3); 58.03 ($NCHCH_2$); 67.57 ($PhCH_2O$); 126.41 (=CH); 127.76, 128.71, 128.95, 129.45 (Ph); 129.64 (CH=); 130.39, 138.16, 138.49 (Ph); 173.34, 173.82, 174.57, 174.93 (CON, CO_2); HRMS: ***m/z*** 553.2662 (MH^+. $C_{29}H_{37}N_4O_7$ requires 553.2660).

4.2.4.2. (E) $PhCH_2OCONHCH(CH_2Ph)CONHCH_2CH{=}CHCH_2CONHCH(CH_3)CONHCH\ (CH_3)CO_2CH_3$ (trans Cbz-Phe-Gly=Gly-Ala-Ala-OCH_3) (3). ^{1}H NMR (DMSO-d_6): δ 1.20 (d, ***J*** = 7.1 Hz, 3H, CH_3(Ala1)); 1.28 (d, ***J*** = 7.3 Hz, 3H, CH_3(Ala2)); 2.76 (dd, ***J*** = 13.4,

10.8 Hz, 1H, CHC***H*****$_2$**Ph); 2.89 (d, ***J*** **=** 5.9 Hz, 2H, CH_2CO); 2.97 (dd, ***J*** **=** 13.6, 4.2 Hz, 1H, CHC***H*****$_2$**Ph); 3.61 (s, 3H, OCH_3); 3.64–3.70 (m, 2H, NCH_2); 4.22 (td, ***J*** **=** 10.3, 4.3 Hz, 1H, NHC***H***CH_2); 4.24 (quintet, ***J*** **=** 7.1 Hz, 1H, CH(Ala2)); 4.31 (quintet, ***J*** **=** 7.3 Hz, 1H, CH(Ala1)); 4.92 (d, ***J*** **=** 12.8 Hz, 1H, PhCH_2O); 4.95 (d, ***J*** **=** 12.8 Hz, 1H, PhCH_2O); 5.45 (dt, ***J*** **=** 15.4, 5.7 Hz, 1H, CH=); 5.60 (dt, ***J*** **=** 15.5, 7.3 Hz, 1H, =CH); 7.18–7.34 (m, 10 H, Ph); 7.52 (d, ***J*** **=** 8.7 1H, NH(Phe)); 8.08 (d, ***J*** **=** 7.6 Hz, 1H, NH(Ala1)); 8.26 (t, ***J*** **=** 5.5 Hz, 1H, N***H***CH_2); 8.40 (d, ***J*** **=** 6.8 Hz, 1H, NH(Ala2)); ^{13}C NMR: δ 16.81 (CH_3(Ala2)); 18.30 (CH_3(Ala1)); 37.9 (CH***C***H_2Ph); 39.5 (***C***H_2CO); 40.4 (NCH_2); 47.48 (CH(Ala2)); 47.62 (CH(Ala1)); 51.84 (OCH_3); 56.27 (N***C***HCH_2); 65.15 (Ph***C***H_2O); 125.44, 129.13 (CH=CH); 126.21, 127.43, 127.65, 128.01, 128.27, 129.22, 137.04, 138.13 (Ph); 155.77 (OCON); 169.65, 171.14, 172.32, 172.96 (CON, CO_2); HRMS: ***m/z*** 553.2680 (MH^+. $C_{29}H_{37}N_4O_7$ requires 553.2660).

4.2.5. Epoxidation

'Pentaeptide' (0.125 mmol), *m*-CPBA 50% (0.218 mmol), K_2HPO_4 (0.181 mmol) were stirred in CH_2Cl_2 (10 ml) and H_2O (10 μl) over night. EtOAc was added (60 ml) and the solution was washed successively with saturated $NaHCO_3$, 5% Na_2SO_3, saturated $NaHCO_3$, water and brine (30 ml each), and dried over $MgSO_4$. Evaporation to dryness afforded the clean product almost quantitatively. The *trans* isomer was purified by chromatography (47:1:2 ethyl acetate/$CHCl_3$/MeOH). A low 27% yield is due to decomposition on the column. Thus, the *cis* product was not purified by chromatography (93% yield).

4.2.5.1. cis PhCH$_2$OCONHCH(CH$_2$Ph)CONHCH$_2$CHOCHCH$_2$CONHCH(CH$_3$)CONHCH(CH$_3$)CO$_2$CH$_3$ (cis Cbz-Phe-Gly-epoxy-Gly-Ala-Ala-OCH$_3$) (4). Diasteriomeric ratio (1:0.6). ^{1}H NMR (CD_3CN): δ 1.29 (d, *J* = 7.2 Hz, 3 H, CHC*H*$_3$ (major)); 1.30 (d, *J* = 7.2 Hz, 3H, CHC*H*$_3$ (minor)); 1.31 (d, *J* = 7.4 Hz, 3H, CHC*H*$_3$ (minor)); 1.32 (d, *J* = 7.2 Hz, 3H, CHC*H*$_3$ (major)); 2.37 (dd, *J* = 15.3, 7.5 Hz, 1H, C*H*$_2$CO (minor)); 2.43 (dd, *J* = 15.3, 6.4 Hz, 1H, C*H*$_2$CO (major)); 2.54 (dd, *J* = 15.3, 6.4 Hz, 1H, C*H*$_2$CO (major)); 2.59 (dd, *J* = 15.1, 5.9 Hz, 1H, C*H*$_2$CO (minor)); 2.86 (dd, *J* = 13.7, 9.2 Hz, 1H, CHC*H*$_2$Ph (major+minor)); 2.90 (m, 1H, NCH_2CHO (minor)); 2.95 (q, *J* = 4.3 Hz, 1H, NCH_2CHO (major)); 3.12 (m, CHC*H*$_2$Ph (major+minor)+NCH_2 (minor)); 3.20 (m, NCH_2 (major)+OC*H*CH_2CO(major+minor)); 3.48 (ddd, *J* = 14.2, 6.5, 5.5 Hz, 1H, NCH_2 (major)); 3.58 (ddd, *J* = 13.8, 6.8, 5 Hz, 1H, NCH_2 (minor)); 3.65 (s, 3H, OCH_3 (minor)); 3.66 (s, 3H, OCH_3 (major)); 4.33 (m, 1H, NHC*H*CH_2); 4.37 (quintet, *J* = 7.3 Hz, 1H, C*H*CH_3); 4.38 (quintet, *J* = 7.3 Hz, 1H, C*H*CH_3); 4.97 (d, *J* = 13 Hz, 1H, PhCH_2O (minor)); 4.97 (d, *J* = 12.1 Hz, 1H, PhCH_2O (major)); 5.04 (d, *J* = 12.6 Hz, 1H, PhCH_2O (minor)); 5.04 (d, *J* = 12.7 Hz, 1H, PhCH_2O (major)); 5.95 (d, *J* = 7.9 Hz, 1H, N*H*CHCH_2 (major)); 6.03 (d, *J* = 8.4 Hz, 1H, N*H*CHCH_2 (minor)); 6.92 (d, *J* = 5.9 Hz, 1H, N*H*CHCH_3 (major+minor)); 6.96 (bd, *J* = 5 Hz, 1H, N*H*CHCH_3 (major)); 7.02 (bd, *J* = 6 Hz, 1H, N*H*CHCH_3 (minor)); 7.22–7.35 (m, 11H, Ph+N*H*CH_2 (major+minor)); ^{13}C NMR: δ 17.69, 17.74, 18.27, 18.29 (CH*C*H_3); 35.56 (*C*H_2CO (minor)); 35.70 (*C*H_2CO (major)); 38.25 (NCH_2 (minor)); 38.48 (NCH_2 (major)); 38.90 (CH*C*H_2Ph); 49.04 (*C*HCH_3 (major)); 49.08, 49.67 (*C*HCH_3 (minor)); 49.74 (*C*HCH_3 (major)); 52.79 (OCH_3 (major)); 52.82 (OCH_3 (minor)); 54.00 (*C*$HOCH_2CO$ (major)); 54.06 (*C*$HOCH_2CO$ (minor)); 54.91 (NCH_2CHO (minor)); 55.13 (NCH_2CHO (major)); 57.45 ($NCHCH_2$ (minor)); 57.53 ($NCHCH_2$ (major)); 67.53 (PhCH_2O); 127.64, 128.55, 128.86, 129.35, 129.37, 129.45, 130.31, 130.33, 138.53 (Ph); 156.95 (OCON) 170.35 (CO_2 (minor)); 170.45 (CO_2 (major)); 172.47 (CON (minor)); 172.54, 173.09 (CON (major)); 174.93 (CON (minor)); HRMS: *m/z* 569.2637 (MH^+. $C_{29}H_{37}N_4O_8$ requires 569.2611).

4.2.5.2. Trans PhCH$_2$OCONHCH(CH$_2$Ph)CONHCH$_2$CHOCHCH$_2$CONHCH(CH$_3$)CONH CH(CH$_3$)CO$_2$CH$_3$ (trans Cbz-Phe-Gly-epoxy-Gly-Ala-Ala-OCH$_3$) (4). Diasteriomeric ratio (1:1). ^{1}H NMR ($CDCl_3$): δ 1.36 (m, 6H, CHC*H*$_3$ (diasteriomers 1+2)); 2.36 (dd, *J* = 15, 6 Hz, 1H, C*H*$_2$CO (1)); 2.39 (dd, *J* = 15, 5.6 Hz, 1H, C*H*$_2$CO (2)); 2.51 (d, *J* = 13.6 Hz, 1H, C*H*$_2$CO (1)); 2.56 (d, *J* = 15.0 Hz, 1H, C*H*$_2$CO (2)); 2.85 (br s, 1H, NCH_2CHO (2)); 2.89 (br s, 1H, NCH_2CHO (1)); 2.97 (m, 1H, OC*H*CH_2CO (1)); 3.00 (m, 1H, CHC*H*$_2$Ph (1+2)); 3.07 (m, OC*H*CH_2CO (2), CHC*H*$_2$Ph (1+2)); 3.23 (m, 1H, NCH_2 (2)); 3.40 (m, 2H, NCH_2 (1)); 3.51 (m, 1H, NCH_2 (2)); 3.70 (s, 3H, OCH_3 (1+2)); 4.49–4.62 (m, 3H, 3× NHC*H* (1+2)); 4.98 (d, *J* = 12.4 Hz, 1H, PhCH_2O (1+2)); 5.05 (d, *J* = 12.4 Hz, 1H, PhCH_2O (1+2)); 6.03 (m, 1H, NH); 7.18–7.39 (m, 13H, Ph+3× NH (1+2)); ^{13}C NMR: δ 17.74, 17.79, 18.38 (CH*C*H_3); 38.38, 38.45 (*C*H_2CO); 38.70, 38.76 (CH*C*H_2Ph); 40.15, 40.26 (NCH_2); 48.19, 48.84, 48.90 (NHCH); 52.48 (OCH_3); 53.03, 53.11 (*C*$HOCH_2CO$); 56.22, 56.26 (NHCH); 56.32, 56.41 (NCH_2CHO); 66.93 (Ph*C*H_2O); 126.93, 127.84, 128.19, 128.50, 128.55, 129.31, 129.73, 130.08, 136.18, 136.51 (Ph); 156.22 (OCON) 168.03, 169.53, 169.59, 172.16, 172.48, 173.17, 173.23 (CO_2+CON); HRMS: *m/z* 569.2581 (MH^+. $C_{29}H_{37}N_4O_8$ requires 569.2611).

4.2.6. Cbz-Phe-Gly-epoxide

The *exo* dipeptidyl epoxide was synthesized from the protected dipeptide Cbz-Phe-GlyOH via the corresponding bromoketone as previously described.[14]

4.2.6.1. PhCH$_2$OCONHCH(CH$_2$Ph)CONHCH$_2$COCH$_2$Br (Cbz-Phe-GlyCH$_2$Br) (5). ^{1}H NMR ($CDCl_3$): δ 2.98 (dd, *J* = 13.5, 7.9 Hz, 1H, CHC*H*$_2$Ph); 3.10 (dd, *J* = 13.8, 5.5 Hz, 1H, CHC*H*$_2$Ph); 3.81 (s, 2H, CH_2Br); 4.13 (dd, *J* = 19.0, 5.0 Hz, 1H, NHC*H*$_2$); 4.21 (dd, *J* = 19.0, 5.0 Hz, 1H, NHC*H*$_2$); 4.59 (q, *J* = 7.3 Hz,1H,CH); 4.97 (d, *J* = 12.3 Hz, 1H, CH_2O); 5.03 (d, *J* = 12.3 Hz, 1H, CH_2O); 5.87 (d, *J* = 8.3 Hz, 1H, NH(phe)); 7.13–7.3 (m, 11H, NH(Gly), Ph); ^{13}C NMR: δ 31.57 (CH_2Br); 38.34 (CH*C*H_2Ph); 46.81 ($NHCH_2$); 55.94 (CH); 66.91 (CH_2O); 126.90, 127.76, 128.05, 128.41, 128.51, 129.15, 136.00, 136.25 (Ph); 156.07 (OCON); 171.78 (CON); 197.47 (CO); HRMS: *m/z* 433.0770 (MH^+. $C_{20}H_{22}N_2O_4Br$ requires 433.0763).

4.2.6.2. PhCH$_2$OCONHCH(CH$_2$Ph)CONHCH$_2$CHOCH$_2$ (Cbz-Phe-Gly-epoxide) (6). ^{1}H NMR ($CDCl_3$): δ 2.28 (dd, *J* = 4.6, 2.7 Hz, 1H, CH_2O (minor)); 2.46 (dd, *J* = 4.1, 2.6 Hz, 1H, CH_2O (major)); 2.62 (t, *J* = 4.1 Hz, 1H, CH_2O (minor)); 2.67 (t, *J* = 4.0 Hz, 1H, CH_2O (major)); 2.90 (m, 1 H, CHO (major)); 2.96 (m, 1H, CHO (minor)); 3.05 (d, *J* = 6.5 Hz, 2H, CHC*H*$_2$Ph); 3.20 (dt, *J* = 14.4, 5.6 Hz, 1H, NHC*H*$_2$ (major)); 3.24 (m, 1H, NHC*H*$_2$ (minor)); 3.56 (ddd, *J* = 14.6, 6.0, 3.0 Hz, 1H, NHC*H*$_2$); 4.44 (dt, *J* = 11.7, 7.0 Hz, 1H, C*H*CH_2Ph); 5.03 (d, *J* = 12.4 Hz, 1H, PhCH_2); 5.06 (d, *J* = 12.4 Hz, 1H, PhCH_2); 5.60 (d, *J* = 8.7 Hz, 1H, NH(Phe) (minor)); 5.62 (d, *J* = 8.0 Hz, 1H, NH(Phe) (major)); 6.38 (m, 1H, NH(Gly)); 7.16–7.33 (m, 10H, Ph); ^{13}C NMR: δ 38.66 (CH*C*H_2Ph); 40.19 ($NHCH_2$ (minor)); 40.32 ($NHCH_2$ (major)); 44.77 (CH_2O (minor)); 44.90 (CH_2O (major)); 50.17 (CHO (minor)); 50.22 (CHO (major)); 56.30 (CHCH_2Ph); 67.01 (PhCH_2); 127.00, 127.95, 128.14, 128.47, 128.61, 129.21, 136.03, 136.30 (Ph); 155.90 (OCON); 171.32 (CON); HRMS: *m/z* 355.1620 (MH^+. $C_{20}H_{23}N_2O_4$ requires 355.1648).

4.3. Inhibition activity

Enzyme kinetics was measured as previously described.[8a]

4.4. Computational modeling

4.4.1. The model construction

Since the epoxy inhibitors occupy both S and S′ subsites in the papain active site, we used the 2cio.pdb file with 1.5 Å resolution[23] as the initial template for the construction of the target non-covalent complexes of our inhibitors with papain. Crystal water and

some co-crystallized solvated small molecules where deleted. The oxidized catalytic Cys25 residue was reduced to thiol. We used the GUI menu commands of Yasara Dynamics software for point mutations in the peptidyl fragments of the original TbICP inhibitor into the desired sequence of the Cbz-Phe-Ψ[Gly-epoxy-Gly]-Ala-Ala-OMe inhibitor. Protecting groups where added. Finally, the epoxide ring was build by the Yasara molecular editor. Hydrogen atoms where added by standard Yasara Dynamics software[20] procedure to the papain–inhibitor complex.

4.4.2. MD simulations

All four papain–inhibitor complexes where optimized in two steps by the Yasara package in Amber99[24] force field. Initially, to release strain caused by the epoxide ring insertion, we optimized the epoxide and its near covalent surrounding—the two $C_\alpha H_2$ fragments. The optimization was conducted in the gas-phase approximation. The rest of the protein–inhibitor complex was frozen. On the next step, a periodic boundary cell was build around the protein–inhibitor complex, 20 Å longer than the corresponding protein axis in each direction. The periodic box was filled with TIP3P explicit water molecules. The whole system was neutralized by adding counter ions and all ionizable protein groups were protonated according to their tabulated pK_a values at pH 7 of the medium. Water molecules were relaxed by simulated annealing procedure. Then we optimized the whole system—the papain–inhibitor complex, water molecules, and counter ions. Minimization was run until the maximum atom speed dropped below 2200 m/s. Then the system was heated from 0 to 298 K. Finally, a short 100 ps molecular dynamics (MD) equilibrated simulation was conducted at 298 K and constant pressure. Multiple time steps were used: 1.25 fs for intramolecular and 2 × 1.25 fs for intermolecular forces. The cutoff was 7.86 Å for van der Waals interactions. The electrostatic interactions were calculated without cutoff by particle mesh Ewald algorithm.[25] Snapshots were collected every 1 ps.

4.4.3. Binding energy calculation

In the post processing analysis of the MD simulation trajectory, the averaged overall snapshots structure of the papain–inhibitor complex was generated as a pdb file. By this way, the generated average structures of all four papain–inhibitor complexes were optimized in the periodic cell with explicit TIP3P water molecules simulating water solvation. Then we extracted a molecular sub-cluster from each of the four enzyme–inhibitor complexes. Every molecular sub-cluster contains the corresponding isomer of the inhibitor and all residues satisfying the condition that there is at least one enzyme–inhibitor atomic pair with a distance <5 Å. Open valences at amine and carboxyl carbon ends were capped by acetylation and protonation, respectively. The newly added acetyl capping groups and all hydrogen atoms of the molecular clusters where optimized in the Amber99 force field in the gas-phase approximation, while all other cluster fragments were kept at the conformations of the previous optimization.

Each of these molecular sub-clusters was separated into two constituting structural components, the protein and the inhibitor, keeping their binding conformation as in the original complex. The binding energy, E_{bind} for every inhibitor was calculated as:

$$E_{bind} = E_{complex} - E_{protein} - E_{inhibitor} \quad (1)$$

The values of $E_{complex}$, $E_{protein}$, and $E_{inhibitor}$ are total energies of the corresponding molecular sub-clusters calculated in the frozen geometry of gas-phase approximation by semiempirical quantum mechanics (QM) by the RM1 Hamiltonian[26] implemented in the Mopac 2007 package.[27]

Acknowledgments

This work was supported by The Israel Science Foundation (Grant No. 1115/04) and by the 'Marcus Center for Pharmaceutical and Medicinal Chemistry' at Bar Ilan University.

Supplementary data

Supplementary data associated with this article can be found, in the online version, at doi:10.1016/j.bmc.2008.08.031.

References and notes

1. (a) Steverding, D.; Caffrey, C. R.; Sajid, M. *Mini-Rev. Med. Chem.* **2006**, *6*, 1025; (b) Vicik, R.; Busemann, M.; Baumann, K.; Schirmeister, T. *Curr. Top. Med. Chem.* **2006**, *6*, 331; (c) Roberts, R. *Drug News Perspect.* **2005**, *18*, 605; (d) Leung-Toung, R.; Zhao, Y.; Li, W.; Tam, T. F.; Karimian, K.; Spino, M. *Curr. Med. Chem.* **2006**, *13*, 547; (e) Neffe, A. T.; Abell, A. D. *Curr. Opin. Drug Discov. Devel.* **2005**, *8*, 684; (f) Turk, B.; Turk, D.; Salvesen, G. S. *Med. Chem. Rev. Online* **2005**, *2*, 283; (g) Ray, S. K. *Proteases Biol. Dis.* **2005**, *3*, 63; (h) Abbenante, G.; Fairlie, D. P. *Med. Chem.* **2005**, *1*, 71; (i) Rosenthal, P. J. *Int. J. Parasitol.* **2004**, *34*, 1489; (j) Lall, M. S.; Jain, R. P.; Vederas, J. C. *Top. Med. Chem.* **2004**, *4*, 1239.
2. Berger, A.; Schechter, I. *Philos. Trans. R. Soc. London, Ser. B* **1970**, *257*, 249.
3. (a) Turk, D.; Guncar, G.; Podobnic, M.; Turk, B. *Biol. Chem.* **1998**, *379*, 137; (b) Storer, A. C.; Ménard, R. *Perspect. Drug Discov. Des.* **1996**, *6*, 33.
4. (a) St. Hilaire, P. M.; Willert, M.; Juliano, M. A.; Juliano, L.; Meldal, M. J. *Comb. Chem.* **1999**, *1*, 509–523; (b) Garcías-Echeverría, C.; Rich, D. H. *FEBS Lett.* **1992**, *297*, 100–102; (c) Garcías-Echeverría, C.; Rich, D. H. *Biochem. Biophys. Res. Commun.* **1992**, *187*, 615–619.
5. (a) Shaw, E. *Adv. Enzyme* **1990**, *63*, 271; (b) Rich, D. H.. In *Proteinase Inhibitors Research Monographs in Cell and Tissue Physiology*; Barrett, A. J., Salvesen, G., Eds.; Elsevier: Amsterdam, 1986; Vol. 12, pp 153–178; (c) Albeck, A. *Drug Dev. Res.* **2000**, *50*, 425; (d) Otto, H.-H.; Schirmeister, T. *Chem. Rev.* **1997**, *97*, 133.
6. (a) Baggio, R.; Shi, Y.-Q.; Wu, Y.-q.; Abeles, R. H. *Biochemistry* **1996**, *35*, 3351; (b) Hu, L.-Y.; Abeles, R. H. *Arch. Biochem. Biophys.* **1990**, *281*, 271; (c) Watanabe, D.; Yamamoto, A.; Tomoo, K.; Matsumoto, K.; Murata, M.; Kitamura, K.; Ishida, T. *J. Mol. Biol.* **2006**, *362*, 979; (d) Stern, I.; Schaschke, N.; Moroder, L.; Turk, D. *Biochem. J.* **2004**, *381*, 511; (e) Marquis, R. W.; Yamashita, D. S.; Ru, Y.; LoCastro, S. M.; Oh, H.-J.; Erhard, K. F.; DesJarlais, R. L.; Head, M. S.; Smith, W. W.; Zhao, B.; Janson, C. A.; Abdel-Meguid, S. S.; Tomaszek, T. A.; Levy, M. A.; Veber, D. F. *J. Med. Chem.* **1998**, *41*, 3563; (f) Yamashita, D. S.; Smith, W. W.; Zhao, B.; Janson, C. A.; Tomaszek, T. A.; Bossard, M. J.; Levy, M. A.; Oh, H.-J.; Carr, T. J.; Thompson, S. K.; Ijames, C. F.; Carr, S. A.; McQueney, M.; D'Alessio, K. J.; Amegadzie, B. Y.; Hanning, C. R.; Abdel-Meguid, S.; DesJarlais, R. L.; Gleason, J. G.; Veber, D. F. *J. Am. Chem. Soc.* **1997**, *119*, 11351; (g) Powers, J. C.; Asgian, J. L.; Ekici, O. D.; James, K. E. *Chem. Rev.* **2002**, *102*, 4639.
7. (a) Leung, D.; Abbenante, G.; Fairlie, D. P. *J. Med. Chem.* **2000**, *43*, 305; (b) Babine, R. E.; Bender, S. L. *Chem. Rev.* **1997**, *97*, 1359; (c) Rich, D. H.. In Hansch, C., Sammes, P. C., Taylor, B. J., Eds.; Comprehensive Medicinal Chemistry; Pergamon Press: Oxford, 1990; 2,. pp 391–441 (d) Lee, C. S.; Choy, N.; Park, C.; Choi, H.; Son, Y. C.; Kim, S.; Ok, J. H.; Yoon, H.; Kim, S. C. *Bioorg. Med. Chem. Lett.* **1996**, *6*, 589.
8. (a) Albeck, A.; Fluss, S.; Persky, R. *J. Am. Chem. Soc.* **1996**, *118*, 3591; (b) Albeck, A.; Kliper, S. *Biochem. J.* **1997**, *322*, 879; (c) Albeck, A.; Kliper, S. *Biochem. J.* **2000**, *346*, 71.
9. Frlan, R.; Gobec, S. *Curr. Med. Chem.* **2006**, *13*, 2309.
10. Allan, R. D.; Dickenson, H. W.; Johnston, G. A. R.; Kazlauskas, R.; Tran, H. W. *Aust. J. Chem.* **1985**, *38*, 1651.
11. Perlman, N.; Albeck, A. *Synth. Commun.* **2000**, *30*, 4443.
12. Perlman, N.; Livneh, M.; Albeck, A. *Tetrahedron* **2000**, *56*, 1505.
13. Shu, L.; Shi, Y. *Tetrahedron* **2001**, *57*, 5213.
14. Albeck, A.; Persky, R. *Tetrahedron* **1994**, *50*, 6333.
15. Segel, I. H. *Biochemical Calculations*, 2nd ed.; Wiley: New York, 1976. pp 246–252.
16. Berti, P. J.; Faerman, C. H.; Storer, A. C. *Biochemistry* **1991**, *30*, 1394.
17. A similar change in the inhibition mechanism for *exo* peptidyl epoxides and the serine protease chymotrypsin has been observed: Kim, D. H.; Li, Z.-H.; Lee, S. S. *Bioorg. Med. Chem. Lett.* **1996**, *6*, 2837.
18. Demarcus, M.; Ganadu, M. L.; Mura, G. M.; Porcheddu, A.; Quaranta, L.; Reginato, G.; Taddei, M. *J. Org. Chem.* **2001**, *66*, 697.
19. Kollman, P.; Massova, I.; Reyes, C.; Kuhn, B.; Huo, S.; Chong, L.; Lee, M.; Lee, T.; Duan, Y.; Wang, W.; Donini, O.; Cieplak, P.; Srinivasan, J.; Case, D. A.; Cheatham, T. E., III *Acc. Chem. Res.* **2000**, *33*, 889.
20. Krieger, E.; Koraimann, G.; Vriend, G. *Proteins* **2002**, *47*, 393. http://www.yasara.com/.
21. Nikitina, E.; Sulimov, V.; Grigoriev, F.; Kondakova, O.; Luschenkina, S. *Int. J. Quant. Chem.* **2006**, *106*, 1943.
22. Krebs, K. G.; Heusser, D.; Wimmer, H. In *Thin Layer Chromatography*; Stahl, E., Ed.; Springer Verlag: New York, 1969; p 862.
23. Alphey, M. S.; Hunter, W. N. *Acta Cryst.* **2006**, *F62*, 504.

24. Wang, J.; Cieplak, P.; Kollman, P. A. *J. Comput. Chem.* **2000**, *21*, 1049.
25. Essman, U.; Perera, L.; Berkowitz, M. L.; Darden, T.; Lee, H.; Pedersen, L. G. *J. Chem. Phys.* **1995**, *103*, 8577.
26. Rocha, G. B.; Freire, R. O.; Simas, A. M.; Stewart, J. J. P. *J. Comp. Chem.* **2006**, *27*, 1101.
27. MOPAC2007, Stewart, J. J. P.; Stewart Computational Chemistry: Colorado Springs, CO, USA, http://OpenMOPAC.net, 2007.